The Promoting Effect of Intermittent Fin Oscillation on the Directional Escape Behavior of Robotic Dolphins

M. N. Hosain[1*], M. E. R. Ekra[2], M. I. Hossain[3], M. D. Ibrahim[4]

[1,2,3,4]School of Electronic and Information Engineering, Nanjing University of Information Science & Technology, Nanjing, China
[*]corresponding author's email: mdnadimhosain@nuist.edu.cn

Abstract – *This paper explores how intermittent fin oscillation can enhance the directional escape behavior of robotic dolphins. As underwater robots take on increasingly important roles in areas like marine research, environmental surveillance, and rescue operations, the limitations of conventional propulsion systems such as high energy use and disruptive noise are becoming more apparent. Unlike traditional propellers, dolphins use oscillatory fin motions to move swiftly and quietly through water, providing inspiration for more efficient and agile underwater robot design. Drawing from this biological model, a bionic robotic dolphin was developed and analyzed using Computational Fluid Dynamics (CFD) simulations. The impact of frequency, amplitude and phase on system performance was studied. The results indicate that when the fins were finely adjusted, the robotic dolphin achieved improved maneuverability* the robotic dolphin achieved improved maneuverability*, spent less energy and moved through the water more efficiently when during rapid escape maneuvers. Flow field visualizations, including pressure distributions and 3D vortex structures, helped explain the mechanisms behind these improvements. Altogether, the research lays groundwork for designing quieter, smarter, and more efficient underwater robots that mimic marine life for applications in underwater surveillance, ecological research, and communication*.

Keywords*: Bio-Inspired Robotics, Escape behavior, Intermittent fin motion, Robotic dolphin, Underwater propulsion,*

Article History
Received 12 April 2026
Received in revised form 20 July 2026
Accepted 06 August 2026

I. Introduction

Underwater robots are now used in many different marine-related activities. They are applied to ocean exploration, environmental monitoring, underwater archaeology, military surveillance and search and rescue operations [1]. The main reason they are important is that the underwater world is usually too risky, deep or complicated for humans to explore for a long time. Thanks to underwater robots, scientists and engineers can visit these difficult areas to gather information, observe marine life, measure pollution and inspect or repair things underwater. Therefore, underwater robots are useful for both research and practical activities in the ocean [2]-[4]. Most underwater robots are either Remotely Operated Vehicles (ROVs) or Autonomous Underwater Vehicles (AUVs). ROVs are linked to a surface ship by cables and are operated by people on the surface [5]. They are often employed in the oil and gas industry to inspect underwater equipment, maintain pipelines and look for new resources. Alternatively, AUVs can function on their own without requiring human supervision. They are commonly used for long-term monitoring or mapping because they can follow set routes and collect data with their sensors. Traditional underwater robots are useful, but their movement system has some limitations [6]. Propellers or thrusters are the main tools used by these robots to move in water [7]. Even though these systems are simple to operate and function well in calm weather, they do have some issues. First, the noise from propellers can bother marine animals and alter the environment beneath the water. This is a major issue in places where being silent is crucial such as in ecological studies or military operations. Propeller-driven robots use a lot of energy, especially when they need to move fast or do difficult tasks. Since they consume a lot of energy, these robots can only work underwater for a limited time, mainly in places where recharging is not convenient. Third, because of their propellers, these robots find it hard to move precisely in areas with obstacles, narrow spaces or strong currents. These limitations indicate the need for

This is an Open Access article distributed under the terms of the Creative Commons Attribution-Noncommercial 3.0 Unported License, permitting copy and redistribution of the material and adaptation for commercial and uncommercial use.

new propulsion methods to move underwater vehicles that are quieter, more efficient and can handle different underwater situations [8]. Nature provides us with many solutions for these engineering issues. Dolphins have a unique and interesting way of swimming, being known for speed and agility while using less energy than other creatures that swim under water [9]. While robotic underwater vehicles use turning blades, dolphins use the manipulation of their fins and tails; fin oscillation is quiet and supports quick, sharp turns that are important for escaping in the wild, where dolphins can swiftly change direction and behave in surprising ways to escape [10]. Their sleek bodies help them move through water efficiently, motivating engineers and scientists to investigate how dolphin movement can be imitated by underwater robots. In particular, this work focuses on intermittent periodic fin oscillation, where fins are active sometimes and rest or glide sometimes, which has been observed in real dolphins and is believed to help them relax and use less energy [11].

This paper examines how making fin movements intermittently in robotic dolphins can guide them in a certain direction [12]. The goal is to create a system that helps the robotic dolphin swim like a real dolphin, making it more flexible and quicker in the water, by studying how the speed, strength and timing of fin movement affect fast and accurate turning during escape [13]. Compared with continuous oscillation, intermittent oscillation includes short breaks between each active movement; by taking these breaks, the vehicle can move forward while using less energy [14]. The aim is to adjust motion settings so the robotic dolphin can respond quickly to obstacles with minimum energy use, enabling efficient and reliable long-period operation in changing conditions [15]. This strategy can also reduce noise: since fin oscillation is less noisy than motorized thrusters, robotic dolphins could be used in sensitive areas without disturbing marine life, which is especially important in ecological surveillance and marine biology studies [16]. By means of mechanical design, motion control and simulation analysis, this work aims to support the development of new bio-mimetic underwater robots that can work in complicated tasks and real-world underwater environments more efficiently and with low power [17].

Accordingly, the main research question is how intermittent fin oscillation can improve the escape maneuvers of robotic dolphins. In nature, dolphins avoid predators or humans through quick, accurate motion using coordinated tails and flippers, yet such escape behaviors remain challenging to replicate: propeller or jet-driven robots are often not fast enough for emergencies and can be ineffective in small, dynamic or unpredictable underwater environments due to high energy consumption, long time delays and big turning radiuses [18]-[20]. This study therefore clarifies key oscillation parameters-frequency, amplitude and phase difference-and links them to thrust, responsiveness, energy consumption and mechanical stress, which can be tuned toward realistic, energy-efficient and safe robotic swimming with a natural tail beat. Because biological swimmers stop fin motion briefly before restarting, accurate control logic is required to decide when fins should be turned on or off, helping batteries last longer and reducing energy use [21], [22]. To connect oscillation-based propulsion with robot motion and energy usage, the work examines water flow, vortex production and pressure distribution using Computational Fluid Dynamics (CFD), and considers how fin design, placement and make affect turning performance, alongside actuator delays and mechanical wear and whether soft robotics and flexible materials might enable dolphin-like swimming [23]. Its main objectives are to: (i) study how fin oscillation influences turning, acceleration, stability, and control delay; (ii) simulate hydrodynamic forces to assess thrust, lift, drag, and vortices, identify effective oscillation frequencies, and evaluate how timing and fin shape affect flow behavior; (iii) use FEA to investigate structural stress during rapid motion; and (iv) apply these results to improve robot shape, fin position, operation, and stiffness, then verify robustness through simulation and tank testing. The expected contribution is a more natural and intelligent control strategy that improves agility, responsiveness, and energy efficiency, while reducing environmental disturbance and supporting reliable data collection and safer ocean technologies.

II. Related Works

Underwater robotics has emerged as a crucial and rapidly advancing field because many aquatic environments are too deep, hazardous, or inaccessible for human intervention, and robots are now essential for marine biology, oceanography, offshore energy exploration, underwater archaeology, naval defense and disaster response; as ocean ecosystem protection increases, aquatic robots have become invaluable tools for researching and working in the ocean [24].

The world's underwater robots mainly fall into two categories: ROVs and AUVs, and although their features and control methods differ, both are required for undersea missions. These types: ROVs are tethered and can operate for a long time with great accuracy, while AUVs are independent for long-distance tasks; underwater robots serve research and industry, where ROVs investigate underwater areas, AUVs support environmental monitoring, Hybrid ROVs carry sensors for deep-sea exploration, and Advanced ROVs conduct geological surveys in tough underwater environments [25].

In practice, ROVs are tethered to research vessels, which provide power and continuous communication.

Equipped with cameras, sonar, robotic arms, and sensors, they are widely used for pipeline inspection, deep-sea exploration, and ship salvage, offering long-duration and highly reliable operation [26]. However, the tether restricts movement, may become entangled, and increases mission cost because specialized vessels and crew are often required. In contrast, AUVs operate without a surface connection, relying on onboard power and sensors for seabed mapping, long-term monitoring, habitat exploration, and access to confined or deep regions. Their limitations include battery life, lack of real-time underwater communication, delayed data retrieval, and the need for advanced autonomy in complex environments. For both systems, conventional propeller- or thruster-based propulsion remains a major weakness because it is noisy, energy intensive, and unsuitable for precise movement in delicate spaces [27]-[29]. As a result, bio-inspired propulsion that imitates the quiet and flexible swimming of marine animals is gaining attention for its lower energy use, reduced noise, and improved control. Following this direction, this article investigates dolphin-like intermittent fin motion to enhance the escape ability and control of robotic dolphins through flexible joints, real-time control, and variable fin movement [30].

Bio-inspired robotics is a rapidly developing field that applies biological principles to design robots that are more flexible, energy efficient, and capable of operating in challenging environments. Because they are based on evolutionary adaptations, these robots are often more agile, controllable, and better suited to their surroundings than conventional mechanical systems [31]. In underwater robotics, dolphins, manta rays, and sea turtles provide valuable models for propulsion, balance, and turning through fin or tail oscillation that enables efficient movement with minimal disturbance. Dolphins inspire fast and maneuverable robotic designs, manta rays guide the development of soft and flexible robots for quiet long-term tasks, and sea turtles motivate energy-efficient robots for extended observation missions. Together, these biological models support motion design for a wide range of underwater applications [32].

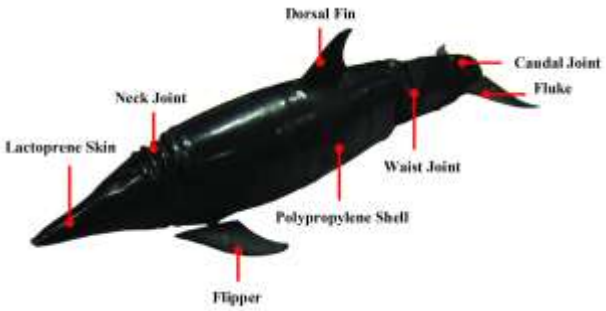


Fig. 1. Single, double, and multi-stage oscillation postures of the robotic dolphin

Biomimetic structures and materials are as important as motion in underwater robots. Soft-bodied or flexibly jointed designs are better suited to unknown, unstructured environments, while advances in soft robotics enable skins and skeletons that function-like muscles and tissues.

Fig. 1 presents a robotic dolphin with neck, waist, and caudal joints, as well as a lactoprene skin and polypropylene shell, allowing dolphin-like bending, fin control, and oscillation-based swimming guidance. Overall, bio-inspired robots can overcome the limits of traditional underwater systems by being quieter, more adaptive, and more environmentally friendly. Based on these ideas, this article seeks to enhance escape performance and power use by imitating marine-animal fin propulsion, thereby supporting sustainable ocean exploration, resource monitoring, and aquatic life protection [33].

When marine animals sense danger or something unexpected, they often try to escape. Dolphins can avoid dangers easily due to their fast movements, flexibility and control, and observing their motion helps design flexible and fast underwater robots [34]. Dolphins respond swiftly and calmly by speeding up fast, turning sharply, and using muscles, tail and fins together, often with unexpected moves that predators struggle to follow. Typically, tail flukes provide propulsion while pectoral fins steer and balance; coordinated fin action and a strong neuromuscular system support rapid maneuvering. Dolphins also swim fast with as little energy as possible due to slippery skin, a bendable backbone and a thin body; tail flukes reduce water breakage and fins stabilize [35]. Their lift-to-drag ratio enables gliding with little energy, and flippers are used in particular ways during escape.

These mechanics and strategies (rolling, diving, spinning) can be captured by high-speed cameras and underwater tracking, revealing water flow near the body and guiding robot designs with flippers, dolphin-type structures and control lines; switching between swimming and finning can save power on long trips. Therefore, dolphins are a strong model for future agile underwater robots [36].

Computational simulation is employed to study the motion of underwater robots in water at low cost. Because underwater experiments are expensive and challenging, simulation methods are increasingly utilized to support continued advancement in the performance, safety and flexibility of robots. In underwater robotics, CFD and FEA are the most common computational tools, and they are fused to study both the interaction between the robot and water and the internal movements of the robot [37]. CFD makes it feasible to simulate how water flows and how fluid forces act on a structure, so researchers can study flow around the robot and its fins and analyze pressure, water resistance, lift and thrust. This helps identify the optimal robot shape, fin motion and swimming patterns so the vehicle can be directed more easily, expend less energy and maintain a steady position. CFD also allows different propulsion approaches-including nature-inspired methods-to be assessed without

building hardware, which is optimal for finned robots with flexure oscillation frequency-dependent motion that can swim such as dolphins; optimal control settings can be derived by testing different frequencies, amplitudes and motion phases [38]-[40].

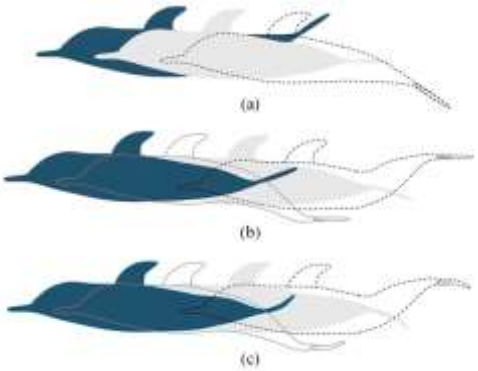


Fig. 2. Body configurations during three dolphin-inspired propulsion modes: (a) Single-stage, (b) Double-stage and (c) Multi-stage

Fig. 2 presents the three main propulsion modes used in robotic dolphin design: (a) single-stage, (b) double-stage, and (c) multi-stage, which represent key elements of dolphin swimming and provide a basis for CFD analysis of tail-fin dynamics. While CFD examines external flow behavior, FEA focuses on internal mechanics by analyzing how fins, joints, and actuators respond to hydrodynamic, mechanical, vibration, and pressure loads. This is important for preventing fatigue and failure, especially during rapid escape movements or in unstable flow conditions. FEA also helps determine whether flexible fins need reinforcement and supports the selection of suitable materials, thickness, and shapes for long-term reliability. Studies in marine biology have shown that efficient swimming in fish, manta rays, and dolphins depends on pressure differences and coordinated body-tail motion, and CFD has helped engineers develop robots with dolphin-like speed and maneuverability [41]. At the same time, FEA has been applied to identify weak points in fish- and dolphin-inspired fin systems and improve structural strength. Together, CFD and FEA allow detailed simulation of fluid and solid behavior, reducing repeated underwater experiments and speeding up the design of durable, animal-like submersible robots.

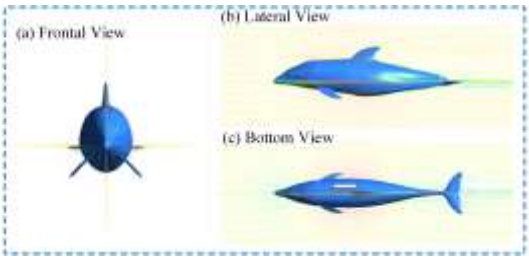


Fig. 3. Streamline visualization around the robotic dolphin from (a) front, (b) lateral, and (c) bottom views

Fig. 3 shows front, side, and bottom streamline views of the robotic dolphin, using vertical and horizontal lines to illustrate water flow around the body. The front view suggests smooth shaping with low resistance, the side view shows largely attached flow near the dorsal and tail regions important for movement, and the bottom view emphasizes flow around the pectoral fins and belly. These results indicate that body size and component placement influence flow and force generation, confirming that a dolphin-like shape supports smooth motion in water.

III. Simulation Model and Methods

A. Bionic Robot Model

The robotic dolphin was designed to imitate a real dolphin so it can move efficiently and naturally in water. Based on biological references, the model remains realistic while being manageable for simulation. Its streamlined body, dorsal fin, pectoral fins, and caudal fluke allow accurate analysis of how fin motion affects directional change, with body length L_b used as the main reference for all other dimensions.

1. Physical Geometry Model

The physical geometry model for the bio-inspired robotic dolphin reduces the complex body of a real dolphin to basic geometric shapes while keeping its main hydrodynamic features.

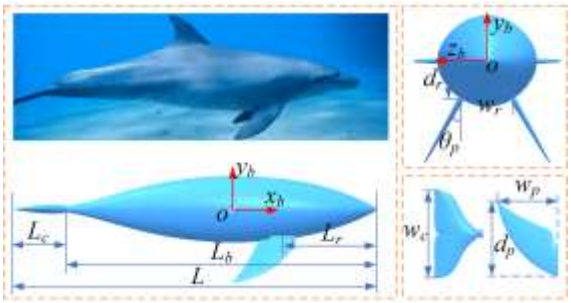


Fig. 4. Geometric model and main dimensional parameters of the bionic robotic dolphin

Fig. 4 presents the physical geometry of the bionic robotic dolphin. Its streamlined body is designed to mimic a real dolphin and reduce water resistance, with the centerline parallel to the x_b axis, and point O located near the center of mass. The body includes two main sections: an elongated elliptical head-trunk part and a tapered caudal peduncle-tail for improved movement.

The main dimensions are the length of the caudal peduncle L_c and the length of the rear body section L_r. L_b is the total body length and is used to normalize all geometric parameters in the simulation so they are consistent and scalable. The pectoral fins, which help with

roll stability and turning, are evenly placed and have width w_p and depth d_p. The dorsal fin is triangular with width w_r and height d_r, mainly helping to prevent rolling. The tail fluke (caudal fin), which helps the fish move forward, is represented by width w_c. The complete geometric parameters and dimensional values used for the bionic robotic dolphin model are summarized in Table I.

TABLE I
GEOMETRIC PARAMETERS AND DIMENSIONS OF THE BIONIC ROBOTIC DOLPHIN

Symbols	Values
$L_b(m)$	2.10
$L_c(m)$	0.36
$w_c(m)$	0.72
$L_r(m)$	0.72
$x_c(m)$	0.96
$w_r(m)$	0.25
$d_r(m)$	0.19
$d_p(m)$	0.44
$w_p(m)$	0.35
$\theta_p(°)$	30

2. Kinematics of Dolphin Robot Escape

The bionic dolphin's self-yaw maneuvering module consists of a flexible main body and a flexible caudal fin, which are described separately to clarify their roles in escape behavior. Like a spine, the dolphin body generates a traveling wave whose amplitude increases from head to tail, enabling coordinated motion for propulsion and turning. To represent this, the traveling-wave motion is combined with a quadratic amplitude envelope containing a constant term, giving the kinematic model of the chordwise flexible body as follows:

$$y_b(x,t) = A(x)\,sin(2\pi ft - kx) \qquad (1)$$

Where $y_b(x,t)$ indicates the momentary sideward displacement of the body, $A(x)$ is an amplitude function described by $A(x) = (C_0 + C_1x + C_2x^2)$, C_0, C_1, and C_2, represent the coefficients that define the amplitude envelope f denotes the frequency of the wave, and k It refers to the wave number that corresponds to the wavelength. It is commonly assumed that the length of the undulating body does not change during wave motion.

Although the body traveling wave drives the boat forward, it does not directly cause turning. Directional change is mainly generated by the lateral motion of the caudal fin, which turns the robotic dolphin through side-to-side translation and oscillation. The lateral movement of the caudal fin near the tail's vertical joint is defined as:

$$y_{cf}(L_b,t) = A_{cf}\,sin(2\pi ft - kL_b) \qquad (2)$$

where A_{cf} refers to the vertical height at the tail's joint, and L_b It refers to the overall length of the dolphin. The swing's lateral flexibility is a type of motion that has a specific phase shift as it moves along the span. The pitching motion of the caudal fin along the spanwise axis has phase shifts that are linearly distributed across the same chordwise line $\theta(t)$ is expressed as:

$$\theta(t) = \theta_{max}\,sin(\omega t - kL_b - \varphi + \delta) \qquad (3)$$

Where θ_{max} is the maximum angle, the caudal fin moves up and down, φ is the phase difference between the side movement and the pitching movement and δ is the angle the caudal fin bends. When $\delta = 0$, the caudal fin acts like a flat plate and does not bend from side to side. All parts of the caudal fin move at the same frequency f and reach the same maximum rotation angle θ_{max}, max can be expressed as:

$$\theta_{max} = \frac{\left[tan^{-1}\left(\frac{A_{cf}\omega}{c}\right) - \alpha_{max}\right]}{sin(\varphi)} \qquad (4)$$

where c is the speed of the body wave, α_{max} is the maximum angle at which the caudal fin moves.



Fig. 5. Caudal-fin phase variation during upward and downward escape maneuvers

Fig. 5 shows the displacement of the caudal fin for different swimming directions. When the fish swims up, its caudal fin goes up, and its body goes down, and when the fish swims down, its body goes up and its caudal fin goes down. They describe the most common ways the fish uses its fins to escape harm in water, maintaining balance, stability, and controlled motion during rapid escape maneuvers.

3. Analysis of Dolphin Robot Posture

A typical 6-DOF rigid body motion model is assumed to analyze and simulate the spatial motion of the robotic dolphin during escape, providing the mathematics for

motion in all three dimensions (translation and rotation). Unlike the biological waveform-based swimming models, this model describes the overall pose and motion of the robotic dolphin using traditional robotics methods. The pose is defined by a 6-DOF configuration vector:

$$q = [x\ y\ z\ \phi\ \theta\ \psi]^T \quad (5)$$

Here, x, y, z are the Cartesian coordinates of the center of mass and ϕ, θ, ψ are the roll, pitch and yaw angles that determine the robot's orientation. They are necessary for controlling the robot's movement and reorientation when it escapes in a liquid environment.

Each link of the robotic dolphin can be described by a homogeneous transformation matrix. Each matrix T_i is defined as:

$$T_i = \begin{bmatrix} R_i & d_i \\ 0 & 1 \end{bmatrix} \quad (6)$$

Where R_i is the 3×3 rotation matrix that encodes the orientation of the i^{th} link or body section, and d_i is the 3×1 position vector representing the displacement from the previous coordinate frame. The complete transformation from the base of the robot to the end-effector (tail) is then obtained by multiplying all the individual segment transformations in order:

$$T = T_1 \cdot T_2 \cdots T_n \quad (7)$$

To model the robot's movement in water, Newton-Euler equations are applied. They describe both straight and rotational motion. Newton's second law explains the translational dynamics:

$$m\frac{d^2r}{dt^2} = F \quad (8)$$

where m is the mass of the robot, r is the position vector of the center of mass, and $F = (F_x,\ F_y,\ F_z)$ represents the resultant external forces acting on the body. The rotational dynamics are given by:

$$J\frac{d^2\omega}{dt^2} = M \quad (9)$$

Here, J is the moment of inertia tensor, ω is the angular velocity vector, and $M = (M_x,\ M_y,\ M_z)$ and is the torque with a traditional tensor formulation with respect to three principal axes. They explain which way the robot is being pushed and spun when it breaks free from the fluid.

The 6-DOF model is also used to predict and control robot responses under different fin oscillations. Together with actuator models and control algorithms, the periodic stroke forces allow the robot body to determine its current motion and orientation, supporting precise control of onboard sensors. To assist positioning and attenuation setting, Fig. 6 (a-f) presents dolphin swimming and leaping postures observed from real movements, including jumping out of the water, sharp turning, and underwater swimming; these postures were analyzed to identify suitable robot positions and angles, and were used to define maximum joint angles, pitch ranges, joint mapping, movement limits, and posture transitions in the simulation model.



Fig. 6. Reference swimming and leaping postures used to define the robotic dolphin's 6-DOF posture transitions

B. Numerical Method

The dolphin was tested in a virtual program by adjusting its settings and speed to determine whether it could move, with the main aim of evaluating how these parameters influence fin turning ability. This process is carried out through simulation. In this study, the flow is assumed to be incompressible and continuous, and the 3D viscous flow around the bionic dolphin is simulated to realistically analyze its motion. Such incompressible flow problems are governed by the Navier-Stokes equations, with conservation of mass and momentum, suitable boundary conditions, and material properties included to ensure stable and physically meaningful numerical results.

1. Governing Equations

The continuity equation is the main equation that ensures mass is not lost or gained:

$$\nabla \cdot u = 0 \quad (10)$$

and the law of conservation of momentum:

$$\rho\frac{\partial u}{\partial t} + \rho(u.\nabla)u = -\nabla p + \mu\nabla^2 u \quad (11)$$

Where ∇ is the gradient operator, ρ is the fluid density, p is the pressure divided by the density, μ is the dynamic viscosity and u is the velocity vector field. Newton's laws of motion are used to describe how the bionic dolphin moves in the water. The dolphin robot's backward and turning movements are shown as:

$$m\frac{d^2r}{dt^2} = \left(F_x, F_y, F_z\right) \quad (12)$$

$$J\frac{d^2\varphi}{dt^2} = (M_x, M_y, M_z) \quad (13)$$

In these equations, (F_x, F_y, F_z) are the fluid forces acting along the three main axes and (M_x, M_y, M_z) are the forces and turning effects on the dolphin's body and pectoral fins in all three directions. In fluid mechanics, the forces and rotations from water can be expressed as follows:

$$(F_x, F_y, F_z) = \iint_s \sigma \cdot n \, dS \quad (14)$$

$$(M_x, M_y, M_z) = \iint_s [(\sigma \cdot n) \times (x - x_c)] \cdot (e_x, e_y, e_z) dS \quad (15)$$

Here, σ is the force acting directly on the dolphin's surface, and n points in the same direction, dS a small area on the dolphin's body (e_x, e_y, e_z) are the basic direction vectors for each principal axis and x_c is the centroid of the dolphin.

Using these equations, this study shows how the dolphin robot moves and reacts, as well as how it escapes under various steering strategies.

2. Computational Domain Setting

A three-dimensional ANSYS Fluent domain is used to model water flow around the bionic dolphin during swimming and to examine its self-yaw and escape behavior under controlled conditions. The rectangular domain is made large enough to reduce boundary effects, with the dolphin placed at the center so the inlet, outlet, and side walls do not artificially affect the flow.

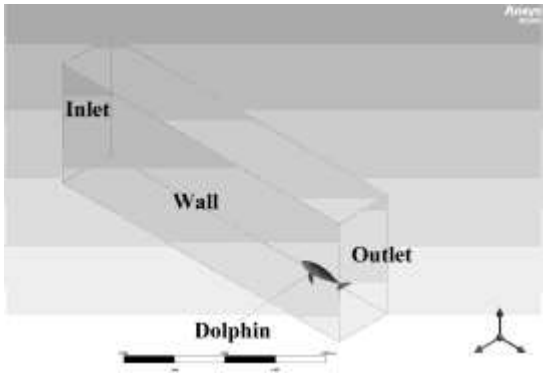


Fig. 7. Computational domain and boundary-condition setup for the bionic robotic dolphin CFD simulation

Fig. 7 shows the three-dimensional computational domain used to simulate the water environment around the bionic dolphin. The inlet applies a fixed velocity, the outlet uses pressure-based discharge, and the top, bottom, and side boundaries are treated as slip or no-slip walls depending on the case. To reduce boundary influence and improve accuracy in self-turning and escape simulations, the dolphin is positioned at the center of the domain. A uniform inflow represents the surrounding water, while the outlet allows fluid to leave freely and avoids backflow. In ANSYS Fluent, the mesh is refined near the dolphin and made coarser farther away to save computation time while still capturing local flow and wider disturbances. These boundary settings are essential for realistic, stable simulation and reliable hydrodynamic and motion results.

3. Flow Field Condition Setting（Numerical Method）

To model fluid motion accurately during robotic dolphin swimming, suitable flow settings must be defined in the computational domain. In this study, the Shear Stress Transport (SST) turbulence model is used because it reliably predicts near-wall flow and flow separation by combining the advantages of the k − ω model near walls with the k − ε model in the free stream. This makes it effective for identifying when flow around the dolphin body may detach and affect motion or steering, while also improving accuracy for rapid water movement both near and away from the body.

A uniform inlet velocity and turbulence level are applied to represent experimental or natural ocean conditions. A pressure outlet prevents instability, while the walls use limited-slip to save computation time or no-slip for improved near-wall accuracy. Water density and viscosity remain constant, and gravity is neglected because inertial and viscous forces dominate at this scale. With body and fin motion tracked throughout the flow, and with the SST model and defined boundaries, the simulation can realistically evaluate how the bionic robotic dolphin moves and escapes in water.

4. Meshing Method

A suitable meshing strategy is required to accurately represent the flow around the bionic dolphin. In this study, the finite element method is used to break the computational domain and dolphin surface into small elements so the fluid dynamic equations can be solved numerically.

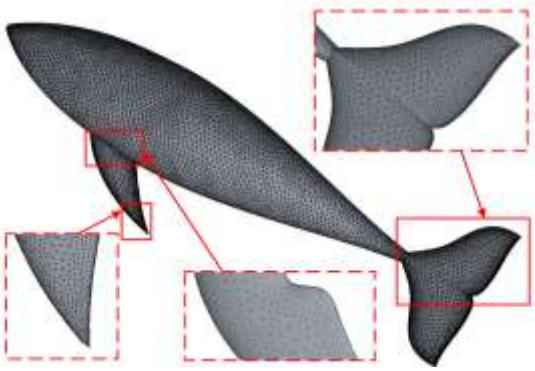


Fig. 8. Surface mesh of the bionic robotic dolphin model with local refinement around the fins and caudal region

Fig. 8 shows the bionic dolphin's surface mesh using

an unstructured triangular grid. Refinement is applied to the pectoral fins, dorsal fin, caudal region, and tail flukes because these areas involve complex geometry and unsteady flow, with extra detail at leading edges and fin tips where velocity and pressure change rapidly. Coarser cells are used in regions with smoother flow to reduce computation time without sacrificing accuracy. Adequate refinement is necessary for representing viscous flow and boundary-layer development, while proper control of skewness, aspect ratio, and mesh transitions ensures quality and solver stability. This mesh therefore enables reliable CFD analysis of dolphin motion and escape behavior in challenging flow conditions.

C. Numerical Validation

The method is validated using a classical case in which a cylinder initially at rest moves vertically in a straight line, confirming its ability to solve 3D locomotion boundary problems and predict fluid forces and flow-field structures. Fig. 9 shows the forces acting on the vibrating cylinder, including the total force, differential component, friction force, and previous reference results, with the red line compared to the black curve reported by Dutsch. Fig. 10 shows the pressure field and vorticity shedding at different phase angles, showing the formation and breakdown of vortex streets, typically dominated by a pair of counter-rotating vortices. These results indicate that the method is suitable for moving-boundary problems such as the cyclo-stationary excitation of a cylinder.

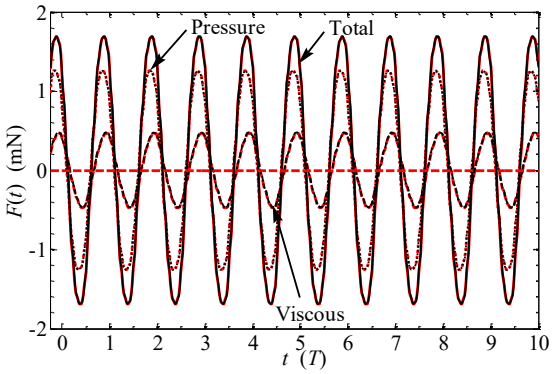


Fig. 9. Comparison of simulated hydrodynamic force components with Dutsch's benchmark results for an oscillating cylinder

Fig. 9 shows how water pressure on the cylinder varies alongside water friction over time. The red results were measured and compared with the benchmark data in black, and both show similar amplitude and phase across many oscillation cycles. This strong agreement between simulation and experiment indicates that the mesh, boundary conditions and turbulence model faithfully capture the key aspects of flowing water, with consistent force trends and reliable temporal behavior under the same oscillatory conditions throughout the test period.

For additional validation, the flow field is examined to verify that the model can reproduce unsteady vortical phenomena such as vortex shedding and wake formation. The resulting vortices and wakes confirm that these behaviors are captured reliably, increasing confidence in the simulation. The predicted vorticity and pressure contours agree closely with experimental fluid-dynamics results, while the visualizations show that different flow structures produce different fluctuation and instability patterns. The model also captures boundary-layer separation and vortex shedding from the moving body, improving realism. When these predictions match measurements, the model can be considered accurate and applied to more complex time-dependent fluid-structure and moving-boundary problems.

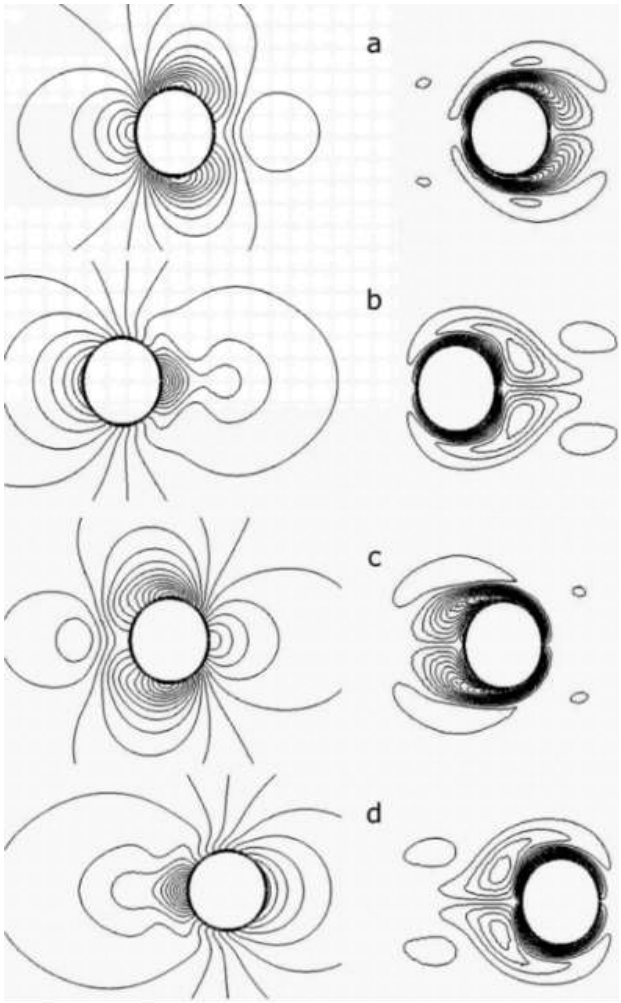


Fig. 10. Pressure and vorticity contours around the oscillating cylinder at four phase angles: (a) γ=0°; (b) γ=96°; (c) γ=192°; (d) γ=288°

Fig. 10 also shows the pressure and vorticity contours around the oscillating cylinder at four different phase angles $\gamma = 0°, 96°, 192°$ and $288°$. The contour plots show that the vortices emerge, evolve and sometimes disappear while shifting in the cylinder. The simulation results coincide with the benchmark, which verifies the numerical method is valid.

After comparing with the measurement results, the simulation is true and reliable and the flow pattern can be observed visually.

IV. Results and Discussion

A. Dolphin Robot Escape Process

The robotic dolphin coordinates body and tail motion to generate the force required for rapid movement and directional change. During escape, it moves forward and upward to imitate real marine animals, as this motion is important for effective evasion. Using the simulation framework introduced earlier, escape-motion data were collected, and the resulting images help explain the robot's movement and fin function, supporting improvements in both design and escape performance.

1. The Escape Trajectory Law

The escape trajectory of the bionic dolphin robot by showing in Fig. 11, which plots the rising displacement P_Y against the forward displacement P_X during the escape maneuver. The curve shows that the robot moves forward and upward at the same time which is part of its self-yaw escape behavior.

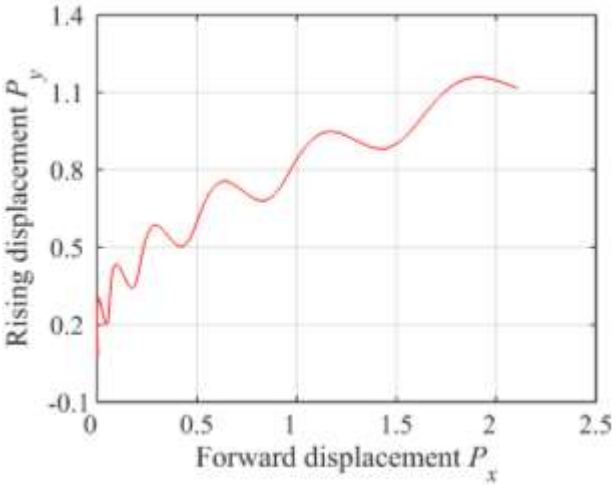


Fig. 11. Relationship between forward displacement P_x and rising displacement P_y during the robotic dolphin escape maneuver

Overall, the trajectory increases steadily with small fluctuations caused by coordinated body and tail-fin motion. In the early stage, these small waves indicate smooth thrust generation, while later larger oscillations suggest stronger coordination between lift and propulsion as the tail moves like that of a real dolphin. The positive slope confirms continuous forward and upward motion, which is essential for underwater escape. The path is not perfectly straight but wavy and S-shaped, resembling the serpentine motion of real dolphins produced by alternating body forces during swimming. This sustained movement demonstrates the benefit of intermittent fin motion for three-dimensional swimming with stable speed and controllable lift. The results therefore confirm the effectiveness of the proposed design, navigation strategy, and control system in reproducing dolphin-like escape behavior.

2. The Variation Pattern of Escape Angle

The pitching angle θ is important during the bionic dolphin robot's escape because it indicates both movement direction and upward capability. By tracking changes in θ, the robot's three-dimensional escape performance can be evaluated.

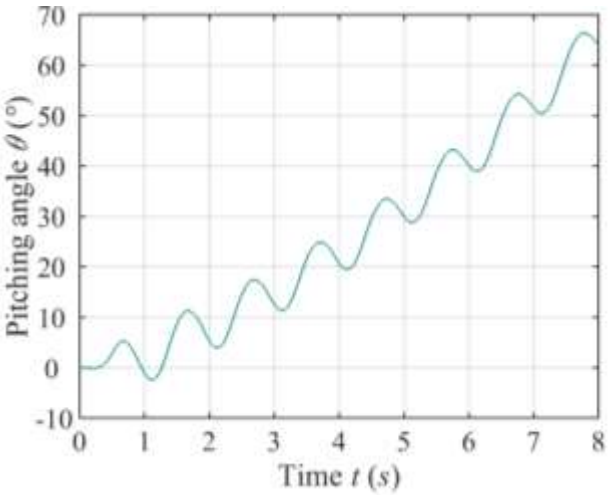


Fig. 12. Time history of pitch angle θ during the robotic dolphin escape maneuver

Fig. 12 shows the time history of θ over 8 s. At the beginning, the robot remains near a neutral angle with small oscillations around zero, corresponding to the initial stage in which the body and caudal fin begin generating thrust and lift. As escape continues, θ increases overall with noticeable fluctuations caused by synchronized body undulation and caudal fin strokes. Around 4 s, the angle reaches about 30°, showing a clear upward climb, and by the end it exceeds 65°, indicating that the robot can quickly leave the horizontal threat zone. This behavior suggests dolphin-like escape motion and confirms that the robot can control its path effectively through pitch regulation.

B. Time History of Performance Parameters

Whilst the dolphin robot escapes, its key kinematic aspects can be observed from the fore-aft and vertical swimming speeds, which agree well with reciprocatory swimming. Examining the velocity history helps infer how propulsion, power input, and control contribute to forward escape motion. Overall, the velocity

characteristics link fin/body movement to swimming direction and confirm the robot achieves the required effectiveness for underwater escape.

1. Time History of Robot Velocity

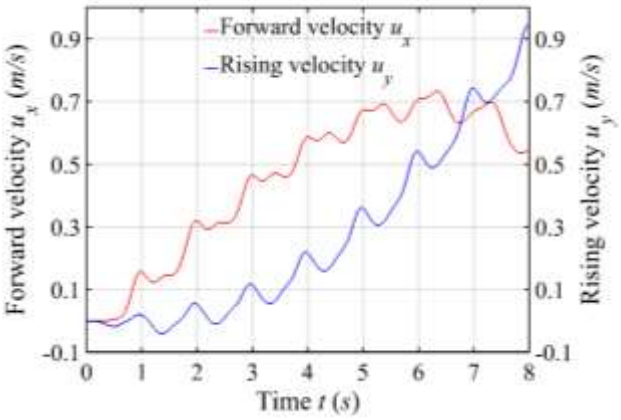


Fig. 13. Time histories of forward velocity u_x and rising velocity u_y during the robotic dolphin escape maneuver

Fig. 13 plots forward velocity u_x (red) and rising velocity u_y (blue) over 8 s of escape. Both start near zero as propulsion begins, then increase with small oscillations from periodic fin/body motion that produces thrust pulses. u_x reaches about 0.7 m/s around mid-escape, while u_y starts lower but steadily builds to roughly 0.7 m/s by the end, showing vertical thrust becomes more important as the robot climbs. Despite cycle-to-cycle speed fluctuations, the overall upward trends indicate stable forward-and-upward motion without loss of control, and the sharp rise near 7 s suggests increased power input similar to a real dolphin's escape response.

2. Time History of Robot Angular Velocity

The angular velocity about the vertical axis ω_z reflects the dolphin robot's ability to perform zigzag turning during escape, since changes in ω_z show how caudal-fin and body motion control turning rate and stabilization. Fig. 14 shows the time history of ω_z over the 8 s escape. ω_z alternates between positive and negative values because body and tail motion generates opposing rotational forces: it rises from zero to a positive peak, then becomes negative after the first oscillation, producing repeated clockwise and counterclockwise yaw. Peak values are about $40°/s$ (positive) and $-25°/s$ (negative), with larger positive peaks indicating a bias toward the escape yaw direction. The oscillation frequency matches the body wave and tail-fin motion, and the nearly constant amplitude/frequency indicate stable, efficient control. Overall, the ω_z history confirms effective rotation control and supports the oscillation-based strategy for dolphin-like 3D escape.

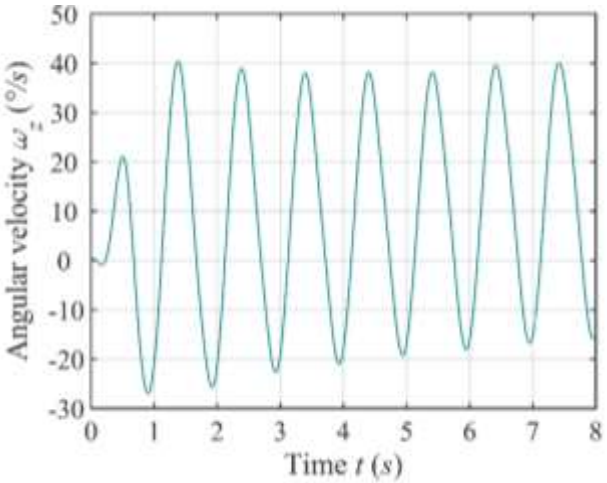


Fig. 14. Time history of yaw angular velocity ω_z during the robotic dolphin escape maneuver

C. Time History of Hydrodynamic Parameters

The escape motion of the bionic dolphin robot is mainly generated by hydrodynamic forces. Analyzing these forces clarifies how the flexible body, oscillating tail, and surrounding water interact during escape, while separating thrust and lift components makes the three-dimensional motion easier to interpret. Such force analysis is therefore essential for improving robot efficiency, movement, and balance.

1. Time History of Forces on the Robot

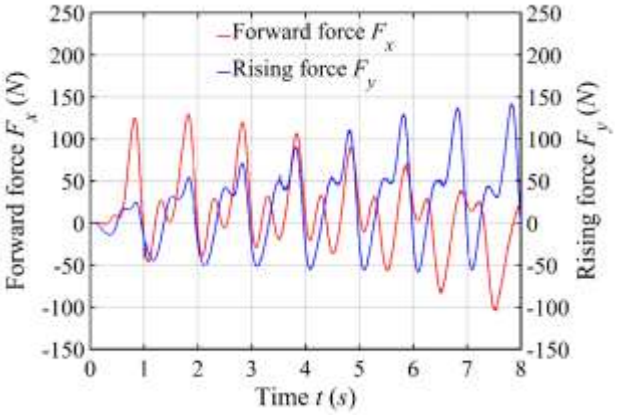


Fig. 15. Time histories of forward force F_x and rising force F_y acting on the robotic dolphin during escape

Fig. 15 shows the hydrodynamic forces on the bionic dolphin robot during the 8 s escape, where the forward force F_x (red) and rising force F_y (blue) indicate how effectively thrust and lift are generated through oscillatory motion. At the beginning, both forces are small, showing

initial body-water interaction, then both magnitudes increase with the periodic body motion and caudal-fin cycles. F_x oscillates strongly with peaks above 100 N and occasional negative dips, reflecting alternating thrust pulses from the caudal-fin stroke and brief reactive intervals that oppose forward motion, as is common in oscillation-based propulsion; however, its overall trend remains positive, confirming sustained forward progression. F_y also oscillates but grows more slowly, reaching a maximum above 100 N after about 5 s as vertical lift strengthens with speed and stability. The similar oscillatory patterns of F_x and F_y confirm combined thrust-lift generation from caudal-fin motion and body deformation, enabling simultaneous forward and upward swimming, and the coordinated high-force response supports the capability of the proposed hydrodynamic approach for fast, dolphin-like escape.

2. Time History of Moment on the Robot

The pitching moment strongly influences the bionic dolphin robot's rotation and controllability during escape, and analyzing it shows how fin actuation and body flexure help the robot change heading and position at high speed.

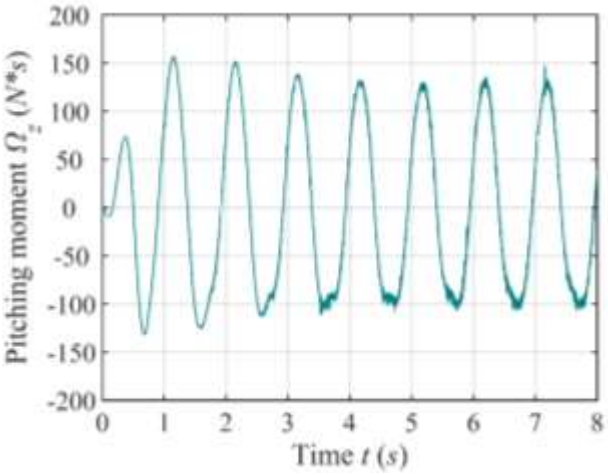


Fig. 16. Time history of pitching moment Ω_z acting on the dolphin robot during escape

Fig. 16 shows the time history of the pitching moment Ω_z during the escape maneuver. The curve rises and falls in an alternating pattern, where each peak changes sign compared with the previous one, because the body and caudal fin oscillate and rotate between successive positions. At the start, Ω_z increases sharply to values well above $100\,\mathrm{N\,.\,s}$, indicating strong initial rotation produced by early caudal-fin motion. It then drops to a negative peak (about -100 to $-150\,\mathrm{N\,.\,s}$) as the tail/fin motion reverses relative to the head and body. This alternating pattern repeats throughout the maneuver with nearly the same frequency and amplitude after the first transient phase. A steady and stable pitching (yaw) moment is necessary to prevent loss of balance or chaotic rotation, and the plot shows that after the first few seconds the moment settles as the robot transitions from a stationary condition to smooth swimming. Once the oscillations become regular, the robot reaches a stable escape state. The alternating positive and negative moments also allow rapid correction of yaw and support selecting an effective three-dimensional escape direction, similar to real dolphins that turn quickly to avoid risks. Overall, the time history indicates that the flexible body and fins enable realistic twisting and dolphin-like swimming during escape.

D. Visualization Results of Dolphin Robot Escape

1. The Pressure Distribution Law on the Dolphin Robot Surface

The escape motion of the bionic dolphin robot can be understood by analyzing hydrodynamic pressure, since thrust, lift and motion depend on pressure variations in time and space. In particular, pressure differences on the caudal fin and soft body are a major driver that guides the robot during escape.

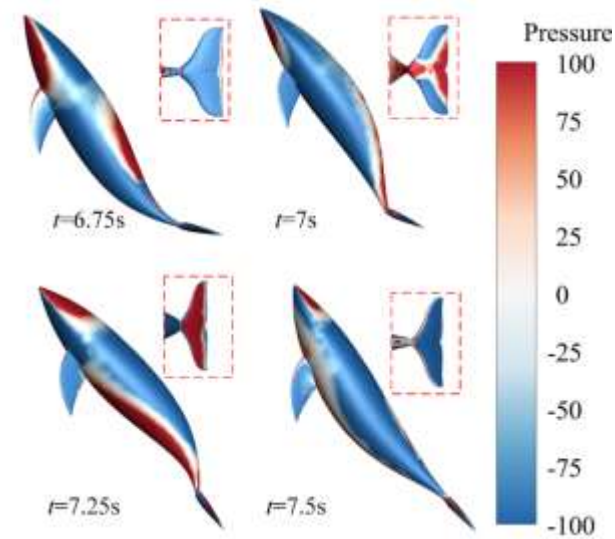


Fig. 17. Surface pressure distribution on the robotic dolphin at various escape instants

Fig. 17 shows surface pressure at $t = 6.75$ s, 7.0 s, 7.25 s and 7.5 s (red: high positive; blue: low/negative), with insets highlighting the caudal fin where propulsion-critical pressure occurs. At $t = 6.75$ s, high pressure is concentrated on the head and leading edges, while negative pressure over the rear body and tail reduces drag; the caudal fin motion pushes the robot forward and pitches the nose upward. At $t = 7.0$ s, pressure shifts toward the caudal fin and decreases near the head, indicating that the tail provides the main forward-and-upward propulsion, and the large tail pressure difference supports improved

propulsion from spanwise flexibility. At $t = 7.25$ s, pressure redistributes along the mid-body and caudal peduncle, with red regions moving along the back and stronger negative pressure at the front, consistent with pitching and upward escape. By $t = 7.5$ s, pressure becomes more uniform and peak values reduce as the robot prepares for the next stroke, while the caudal fin still maintains alternating high/low pressure to sustain thrust during recovery. Overall, the pressure distribution shows that the robot uses local pressure to maintain motion and control heading, with strong zones near joints driving propulsion and low-pressure regions helping manage drag, confirming the effectiveness of the combined fluid-dynamics and biology-style approach.

2. The Pressure Distribution Law of the Flow Field

To explain thrust generation, wake-related disturbances, and swimming speed, the pressure field around the dolphin robot during escape must be examined. The flow field shows the interaction between the fluid and the structure, while boundary-layer pressure plots reveal thrust, lift, wake motion, and vortex shedding, confirming that vibration transfers energy into directed movement.

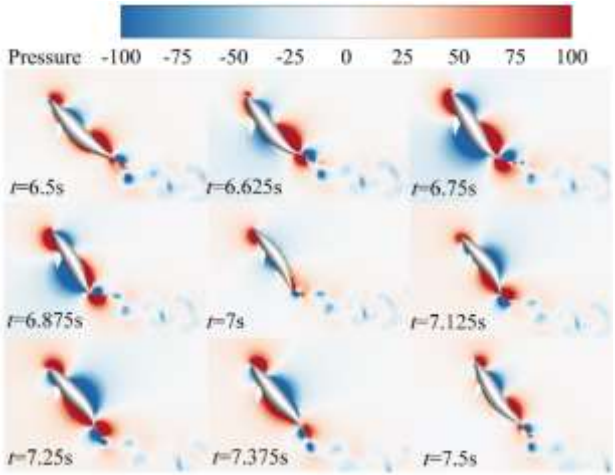


Fig. 18. The pressure distribution in the water around the dolphin robot at various times during its escape

Fig. 18 shows the pressure field around the dolphin robot from $t = 6.5$ s to $t = 7.5$ s (red: high positive pressure, blue: low/negative pressure), illustrating how robot motion drives the surrounding water. At $t = 6.5$ s, a strong high-pressure region forms at the head with low pressure behind the body; the caudal-fin stroke creates a clear pressure difference that pushes the robot forward. At $t = 6.625$ s and $t = 6.75$ s, these high/low regions grow and shift downstream, and alternating positive/negative pressure develops in the wake, indicating vortex generation from body and fin oscillation. At $t = 6.875$ s and $t = 7.0$ s, pressure near the caudal fin intensifies with strong red/blue zones at the tail, showing strong forward motion and shedding of large vortices that support thrust and an organized downstream flow. From $t = 7.125$ s to $t = 7.375$ s, the field enters a recovery phase: pressure magnitudes weaken slightly and the wake forms paired vortices, preparing for the next oscillation cycle. By $t = 7.5$ s, the pressure field becomes more evenly distributed and the wake vortices appear more symmetric, indicating that oscillatory locomotion provides a stabilized, propulsive escape mode. Overall, the flow-field pressure distribution confirms that the bionic dolphin robot regulates surrounding water to generate thrust and lift and to steer, while wake patterns and pressure variations support the bio-inspired swimming principle and demonstrate the robot's capability for three-dimensional escape in water, with coherent pressure gradients evolving smoothly in time, consistent with the repeated fin-stroke sequence, and providing clear evidence of stable flow control during successive phases of the maneuver.

3. The Vorticity Distribution Law of the Flow Field

Vorticity represents fluid rotation, so its distribution around the bionic dolphin robot reveals how important hydrodynamic effects are formed. By analyzing the vorticity field, changes in swimming velocity can be linked to body-tail interaction during escape, while also helping to understand and improve three-dimensional motion, wake development, vortex shedding strength, and their effects on thrust, lift, and overall stability.

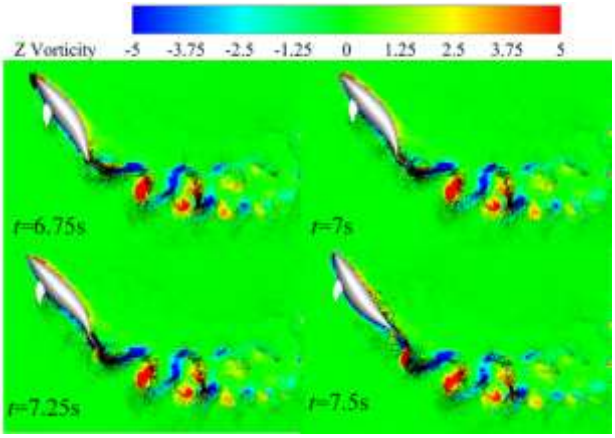


Fig. 19. The distribution of vorticity in the flow field around the dolphin robot at various times during escape

Fig. 19 shows the Z-component of vorticity at $t = 6.75$ s, 7.0 s, 7.25 s and 7.5 s (blue: strong negative, red: strong positive, green: near zero). At $t = 6.75$ s, positive and negative vorticity layers form near the body and tail, and vortices shed downstream to form the initial vortex street; the alternating vorticity in the wake indicates thrust is not constant because fin strokes generate vortices in alternating directions. At $t = 7.0$ s, eddies become clearer and more organized, producing a repeating wake pattern; the symmetry of rotating vortices shows the robot is

controlling itself through coordinated body-and-fin motion. At $t = 7.25$ s, the wake is more organized and vortices interact farther from the body; closely spaced alternating vortices support forward motion with less energy lost to turbulence. By $t = 7.5$ s, the wake shows distinct counter-rotating vortex pairs, and the more even vorticity distribution indicates an efficient system for fast forward-and-upward escape. The whorl-like flow around the dolphin-inspired body demonstrates strong interaction with passing water, and the observed vortex structures confirm that the robot swims underwater in an animal-like way that supports swift and effective escape, as the wake evolves into a consistent, repeatable pattern over time, reflecting stable propulsion cycles and controlled flow organization during the entire escape maneuver.

4. 3D Vortex Structures

A 3D view of vortex structures during escape helps explain the wake in a way that 2D pressure and vorticity plots cannot: while 2D results visualize local flow, the 3D wake describes the interior dynamics of the swimming robot and indicates how effectively it can escape.

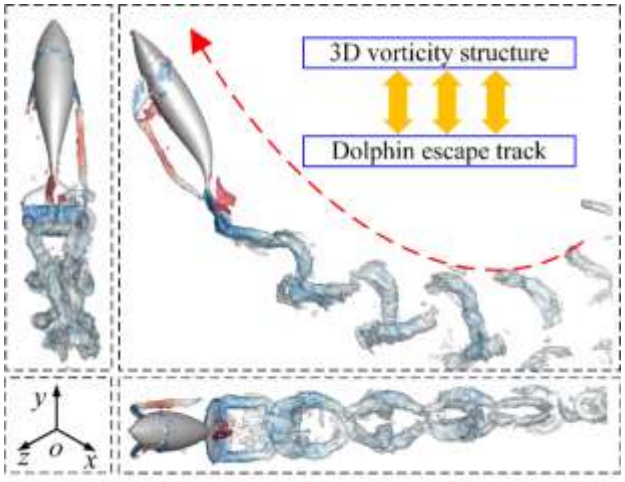


Fig. 20. Three-dimensional vortex structures generated by the robotic dolphin during the escape maneuver

Fig. 20 shows the three-dimensional vortex structures generated as the dolphin robot avoids collision. Iso-surfaces represent vorticity energy, and color distinguishes positive and negative rotation, allowing the wake to be viewed from different angles. From above, a series of vortex rings appears behind the robot, with each caudal-fin stroke releasing a clear eddy into the wake; their regular spacing suggests efficient forward propulsion with little wasted energy. The side view shows that the vortices remain connected to the body and tilt during ascent to support forward and upward motion, while their close spacing suggests effective use of the wake. The rear view reveals symmetrical vortex-loop relaxation, indicating stable rather than irregular swimming. Overall, the 3D vortex pattern shows that the bionic dolphin robot generates an animal-like wake, where well-formed and symmetric vortices correspond to strong thrust, lift, and stable control. This confirms that the flexible body and intermittent tail motion are effective for escape and that vortex shedding remains organized and repeatable throughout the maneuver.

V. Conclusion

This paper investigated how intermittent fin oscillation (periodic flap-up/flap-down with short gliding intervals) can improve the directional escape behavior of a bionic robotic dolphin. A dolphin-inspired geometry with a streamlined body, dorsal and pectoral fins, and a flexible caudal fluke was modeled, and the escape motion was described using a 6-DOF rigid-body framework for overall pose together with flexible-body traveling-wave motion and caudal-fin lateral oscillation to generate turning and climbing. A CFD-based simulation pipeline was established in ANSYS Fluent, including a sufficiently large computational domain, appropriate inlet-outlet-wall boundary conditions, an SST turbulence model, and refined meshing around fins and the caudal region, with reliability supported through a standard moving-boundary validation case. The results show stable three-dimensional escape with simultaneous forward and upward progression: the trajectory increases with oscillatory fluctuations reflecting body-tail coordination, the pitching angle rises from near neutral to a strong pitch-up state, and the forward and rising velocities grow with periodic thrust pulses while maintaining control. Angular-velocity and moment histories show repeatable zigzag yaw behavior and alternating moments that enable rapid correction without instability. Force, pressure, vorticity, and 3D wake visualizations reveal that coordinated body deformation and caudal-fin strokes generate coupled thrust and lift, create organized alternating vortices and coherent vortex-ring structures, and regulate the surrounding flow in a manner consistent with efficient dolphin-like propulsion. Overall, the findings confirm that intermittent fin oscillation and the proposed bio-inspired mechanics and control can reproduce key escape responses and provide a practical basis for agile, energy-aware underwater robots suited to complex and sensitive marine environments.

Conflict of Interest

The authors declare no conflict of interest in the publication process of the research article.

Author Contributions

All authors contributed to the conception and design of this study. Material preparation, data collection, and

analysis were performed by Author 1 and Author 2. Supervision and validation were carried out by Author 1, Author 2, and Author 3. Data organization and comparative analysis were performed by Author 1 and Author 4. The first draft of the manuscript was written by Author 2, and all authors commented on earlier versions of the manuscript. All authors read and approved the final manuscript.

References

[1] X. Li, D. Zhang, M. Zhao, X. Wang, and Y. Shen, "Hydrodynamic Analysis and Drag-Reduction Design of an Unmanned Underwater Vehicle Based on Computational Fluid Dynamics," J. Mar. Sci. Eng., vol. 12, no. 8, p. 1388, Aug. 2024, doi: 10.3390/JMSE12081388.

[2] J. Mirza et al., "Underwater temperature and pressure monitoring for deep-sea SCUBA divers using optical techniques," Front. Phys., vol. 12, p. 1417293, Jul. 2024, doi: 10.3389/FPHY.2024.1417293.

[3] R. Bogue, "Underwater robots: a review of technologies and applications," Industrial Robot: the international journal of robotics research and application, vol. 42, no. 3, pp. 186–191, May 2015, doi: 10.1108/IR-01-2015-0010.

[4] K. Hasan et al., "Oceanic Challenges to Technological Solutions: A Review of Autonomous Underwater Vehicle Path Technologies in Biomimicry, Control, Navigation, and Sensing," IEEE Access, vol. 12, pp. 46202–46231, Mar. 2024, doi: 10.1109/ACCESS.2024.3380458.

[5] J. Xu, X. Irigoien, and M. S. Alouini, "State-of-the-Art Underwater Vehicles and Technologies Enabling Smart Ocean: Survey and Classifications," arXiv preprint arXiv:2412.18667, pp. 1–35, Dec. 2024, doi: 10.48550/arXiv.2412.18667.

[6] C. Yang, X. Wu, M. Lin, R. Lin, and D. Wu, "A review of advances in underwater humanoid robots for human–machine cooperation," Rob. Auton. Syst., vol. 179, p. 104744, Sep. 2024, doi: 10.1016/J.ROBOT.2024.104744.

[7] D. Scaradozzi, G. Palmieri, D. Costa, and A. Pinelli, "BCF swimming locomotion for autonomous underwater robots: a review and a novel solution to improve control and efficiency," Ocean Engineering, vol. 130, pp. 437–453, Jan. 2017, doi: 10.1016/J.OCEANENG.2016.11.055.

[8] B. Windén and H. Kamiirisa, "Underwater Noise Concerns: How Can the Maritime Industry React?," Journal of Ship Production and Design, vol. 40, no. 01, pp. 1–9, Feb. 2024, doi: 10.5957/JSPD.01220002.

[9] G. Tian, D. Fan, X. Feng, and H. Zhou, "Thriving artificial underwater drag-reduction materials inspired from aquatic animals: progresses and challenges," RSC Adv., vol. 11, no. 6, pp. 3399–3428, Jan. 2021, doi: 10.1039/D0RA08672J.

[10] J. C. Liao, "Towards the yin and yang of fish locomotion: linking energetics, ecology and mechanics through field and lab approaches," Journal of Experimental Biology, vol. 228, no. Suppl_1, Feb. 2025, doi: 10.1242/JEB.248011/367023.

[11] Z. Zhang, Q. Wang, and S. Zhang, "Review of Computational Fluid Dynamics Analysis in Biomimetic Applications for Underwater Vehicles," Biomimetics, vol. 9, no. 2, p. 79, Jan. 2024, doi: 10.3390/BIOMIMETICS9020079.

[12] E. Anwar, S. Abeywardena, S. C. Miller, and I. Farkhatdinov, "Design and Validation of a Wearable Robotic Tail for Human Balance Support," in Proceedings of the IEEE RAS and EMBS International Conference on Biomedical Robotics and Biomechatronics, Heidelberg, Germany: IEEE Computer Society, Oct. 2024, pp. 895–900. doi: 10.1109/BIOROB60516.2024.10719748.

[13] A. Anand, M. Yuva Bharath, P. Sundaravadivel, J. Preetha Roselyn, and R. Annie Uthra, "On-Device Intelligence for AI-Enabled Bio-Inspired Autonomous Underwater Vehicles (AUVs)," IEEE Access, vol. 12, pp. 51982–51994, Apr. 2024, doi: 10.1109/ACCESS.2024.3385435.

[14] J. Mirza et al., "Relay aided UWOC-SMF-FSO based hybrid link for underwater wireless optical sensor network," Optical Fiber Technology, vol. 89, p. 104045, Jan. 2025, doi: 10.1016/J.YOFTE.2024.104045.

[15] D. J. Coughlin and M. D. Dutterer, "Intermittent swimming and muscle power output in brook trout, Salvelinus fontinalis," J. Exp. Zool. A Ecol. Integr. Physiol., vol. 341, no. 8, pp. 896–902, Oct. 2024, doi: 10.1002/JEZ.2844.

[16] A. Tomassini et al., "Interpersonal synchronization of movement intermittency," iScience, vol. 25, no. 4, Apr. 2022, doi: 10.1016/j.isci.2022.104096.

[17] L. Jin and W. Cui, "On technical issues for underwater charging of robotic fish schools using ocean renewable energy," Ships and Offshore Structures, vol. 19, no. 9, pp. 1465–1475, Sep. 2024, doi: 10.1080/17445302.2023.2245164.

[18] Z. Yang, W. Gong, H. Chen, S. Wang, and G. Zhang, "Research on the Turning Maneuverability of a Bionic Robotic Dolphin," IEEE Access, vol. 10, pp. 7368–7383, Jan. 2022, doi: 10.1109/ACCESS.2022.3142521.

[19] H. Feng, Y. Zhang, and D. Fan, "Physics-Informed Fine-Tuned Neural Operator for Flow Field Modeling," J. Mar. Sci. Eng., vol. 14, no. 2, p. 201, Jan. 2026, doi: 10.3390/JMSE14020201.

[20] Z. Yu, A. Duan, Z. Zhu, and W. Zhang, "Biomimetic soft-legged robotic locomotion, interactions and transitions in terrestrial, aquatic and multiple environments," Sustainable Materials and Technologies, vol. 40, p. e00930, Jul. 2024, doi: 10.1016/J.SUSMAT.2024.E00930.

[21] S. Tang, Y. Zhu, and S. Yuan, "Bionics-Inspired Structure Boosts Drag and Noise Reduction of Rotating Machinery," J. Bionic Eng., vol. 20, no. 6, pp. 2797–2813, Nov. 2023, doi: 10.1007/S42235-023-00404-3.

[22] P. C. Sternes, L. Schmitz, and T. E. Higham, "The rise of pelagic sharks and adaptive evolution of pectoral fin morphology during the Cretaceous," Current Biology, vol. 34, no. 12, pp. 2764-2772.e3, Jun. 2024, doi: 10.1016/j.cub.2024.05.016.

[23] Y. Feng and Y. Su, "Numerical study of the cruising-maneuvering motion of a fish-like swimmer using the co-propulsion of the caudal fin and pectoral fin under self-propulsion," Physics of Fluids, vol. 37, no. 4, Apr. 2025, doi: 10.1063/5.0263911/3341960.

[24] S. K. Sahoo, B. B. Choudhury, and P. R. Dhal, "Exploring the Role of Robotics in Maritime Technology: Innovations, Challenges, and Future Prospects," Spectrum of Mechanical Engineering and Operational Research, vol. 1, no. 1, pp. 159–176, Jul. 2024, doi: 10.31181/SMEOR11202414.

[25] G. Ioannou et al., "Underwater Inspection and Monitoring: Technologies for Autonomous Operations," IEEE Aerospace and Electronic Systems Magazine, vol. 39, no. 5, pp. 4–16, May 2024, doi: 10.1109/MAES.2024.3366144.

[26] L. Hong, X. Wang, and D. S. Zhang, "CFD-based hydrodynamic performance investigation of autonomous underwater vehicles: A survey," Ocean Engineering, vol. 305, p. 117911, Aug. 2024, doi: 10.1016/J.OCEANENG.2024.117911.

[27] J. Sun, Q. Zhang, Y. Lu, B. Huang, and Q. Li, "A Review of Touching-Based Underwater Robotic Perception and Manipulation," Machines, vol. 13, no. 1, p. 41, Jan. 2025, doi: 10.3390/MACHINES13010041.

[28] J. A. Cardenas et al., "A systematic review of robotic efficacy in coral reef monitoring techniques," Mar. Pollut. Bull., vol. 202, p. 116273, May 2024, doi: 10.1016/J.MARPOLBUL.2024.116273.

[29] Y. Xie, M. E. R. Ekra, T. Gu, and X. Wang, "A Research on Positioning Algorithm Based on RPCA in Sparse Fingerprint Environment," International Journal of Informatics, Information System and Computer Engineering (INJIISCOM), vol. 6, no. 2, pp. 225–245, Feb. 2025, doi: 10.34010/INJIISCOM.V6I2.14980.

[30] Y. A. H. ; ; Li et al., "Recent Advances, Future Trends, Applications and Challenges of Internet of Underwater Things (IoUT): A Comprehensive Review," J. Mar. Sci. Eng., vol. 11, no. 1, p. 124, Jan. 2023, doi: 10.3390/JMSE11010124.

[31] L. Abualigah, X. Xia, A. Alabdulatif, and N. Neranjan Thilakarathne, "Bio-Inspired Internet of Things: Current Status, Benefits, Challenges, and Future Directions," Biomimetics, vol. 8, no. 4, p. 373, Aug. 2023, doi: 10.3390/BIOMIMETICS8040373.

[32] D. Ramakrishna and G. Bala Murali, "Bio-inspired 3D-printed lattice structures for energy absorption applications: A review," in Proceedings of the Institution of Mechanical Engineers, Part L: Journal of Materials: Design and Applications, SAGE Publications Ltd, Mar. 2023, pp. 503–542. doi: 10.1177/14644207221121948.

[33] F. Glaviano et al., "Management and Sustainable Exploitation of Marine Environments through Smart Monitoring and Automation," J. Mar. Sci. Eng., vol. 10, no. 2, p. 297, Feb. 2022, doi: 10.3390/JMSE10020297.

[34] A. M. McGowan et al., "Cryptic marine barriers to gene flow in a vulnerable coastal species, the dugong (Dugong dugon)," Mar. Mamm. Sci., vol. 39, no. 3, pp. 918–939, Jul. 2023, doi: 10.1111/MMS.13021.

[35] V. Y. Nguyen, S. M. Bayse, H. A. Einarsson, and Ó. A. Ingólfsson, "Inferring fish behaviour at the trawl mouth from escape location," PeerJ, vol. 11, p. e14746, Jan. 2023, doi: 10.7717/PEERJ.14746.

[36] R. M. Suhardi et al., "A review of the mangrove ecosystem in Indonesia: Biodiversity, conservation, and challenges in sustainable management," Ecol. Genet. Genom., vol. 32, p. 100282, Sep. 2024, doi: 10.1016/J.EGG.2024.100282.

[37] Z. Yuan, Y. Chang, C. Chen, Y. Chen, and S. Chen, "Calculation of Propulsive Motion for Two-Jointed Bionic Robotic Dolphin," Appl. Bionics Biomech., vol. 2024, no. 1, p. 5978563, Jan. 2024, doi: 10.1155/2024/5978563.

[38] Z. Xue, L. Li, and Y. Song, "The Research of Maneuverability Modeling and Environmental Monitoring Based on a Robotic Dolphin," Appl. Bionics Biomech., vol. 2021, no. 1, p. 4203914, Jan. 2021, doi: 10.1155/2021/4203914.

[39] M. Emadur et al., "Wi-Fi Indoor Location Method based on Improved Fingerprint Technique," European Journal of Electrical Engineering and Computer Science, vol. 9, no. 2, pp. 33–39, Apr. 2025, doi: 10.24018/EJECE.2025.9.2.704.

[40] Z. Zhang, Q. Wang, and S. Zhang, "Review of Computational Fluid Dynamics Analysis in Biomimetic Applications for Underwater Vehicles," Biomimetics, vol. 9, no. 2, p. 79, Jan. 2024, doi: 10.3390/BIOMIMETICS9020079.

[41] Z. Li, M. Lei, S. Jiao, H. Yan, Y. Li, and D. Xia, "Using the windmill-shaped array layout to realize the self-rolling propulsion of a multi-tentacled underwater robot," Ocean Engineering, vol. 331, p. 121352, Jul. 2025, doi: 10.1016/J.OCEANENG.2025.121352.